Journal of Physics and Chemistry of Solids 84 (2015) 85–95

Contents lists available at ScienceDirect

Journal of Physics and Chemistry of Solids

journal homepage: www.elsevier.com/locate/jpcs

Solvated fullerenes, a new class of carbon materials suitable for high-pressure studies: A review

Lin Wang [a,b,c,*]

[a] HPSynC, Geophysical Laboratory, Carnegie Institution of Washington, Argonne, Lemont, IL 60439, USA
[b] State Key Laboratory of Superhard Materials, Jilin University, Changchun 130012, China
[c] Center for High Pressure Science and Technology Advanced Research, 1690 Cailun Rd, Pudong District, Shanghai 201203, China

ARTICLE INFO

Article history:
Received 24 January 2014
Received in revised form
8 June 2014
Accepted 9 June 2014
Available online 18 June 2014

Keywords:
A. Fullerenes
C. High pressure
D. Crystal structure
D. Phase transitions

ABSTRACT

As the list of known carbon compounds grows longer, solvated fullerenes have become a more important class of carbon materials. Their general properties and methods of synthesis have both attracted considerable attention. The study of the behavior of these compounds under high-pressure conditions has revealed several new phenomena that have never been observed in pure fullerene. This article is a review of all recent progress in this field.

1. Introduction

Carbon became one of the most attractive elements in the periodic table during the 1980s. It attracted a great deal of research effort in material science, chemistry, and condensed matter physics. Several new carbon allotropes, including fullerenes (C_{60}, C_{70}, etc.), carbon nanotubes, and graphene have been discovered and subjected to study in the past few decades [1–4]. Within the carbon family, fullerenes have very unique closed-cage structure and can be treated as zero dimensional materials, which have many fascinating properties. The family includes C_{20}, C_{36}, C_{60}, C_{70}, and other compounds [5–9]. They have a wide range of properties and considerable potential in applications such as energy storage and solar cells [10–13].

Pressure is a very important parameter in tuning materials' properties. The distance between atoms, crystal structure, and electronic structure of the atoms can all be modified under high pressure [14–17]. High-pressure structural evaluations of C_{60} and C_{70} have been performed and the polymerization of C_{60} and C_{70} has been widely studied [18–22]. The fullerene molecules themselves are incompressible, but the intermolecular interactions are weak. The C=C bonds also make it possible to generate polymerized phases. These characteristics of fullerenes yield a rich variety of phase transitions under compression conditions and across a wide range of temperatures. Several great reviews of this topic have been made [18–21].

The superconductive properties of alkali-doped fullerenes have made them a hot topic [9,23–25]. The structural stability and superconducting transition temperatures of alkali-doped fullerenes have also been studied thoroughly [24,25]. The fact that fullerenes can generate solvates when they crystallize from solvents is of particular interest [26–29]. Many studies have focused on the growth and characterization of solvated fullerenes [26–45]. High-pressure studies on this kind of fullerene materials have been carried out by several groups [46–57]. High-pressure structural investigations were performed on solvated fullerenes and this family was found to behave very differently from pure and alkali-doped fullerenes. In 2012, Wang et al. discovered a novel long-range ordered material constructed from units of amorphous carbon clusters which was synthesized by compressing solvated fullerenes [58]. After the discovery, this topic has attracted more attentions and a great deal of progress has been made. To emphasize the importance of these materials, the following review of recent studies on solvated fullerenes and their properties, including phase transitions and polymerization under high-pressure conditions, was assembled. This review may interest more research groups in this field.

2. Fullerenes

Closed fullerenes were first predicted by Jones in 1966 [5,59]. He proposed large, hollow, closed-cage molecules constructed

* Correspondence address: HPSynC, Geophysical Laboratory, Carnegie Institution of Washington, Argonne, Lemont, IL 60439, USA.
E-mail addresses: wanglin@hpstar.ac.cn, lwang@carnegiescience.edu

http://dx.doi.org/10.1016/j.jpcs.2014.06.007
0022-3697/

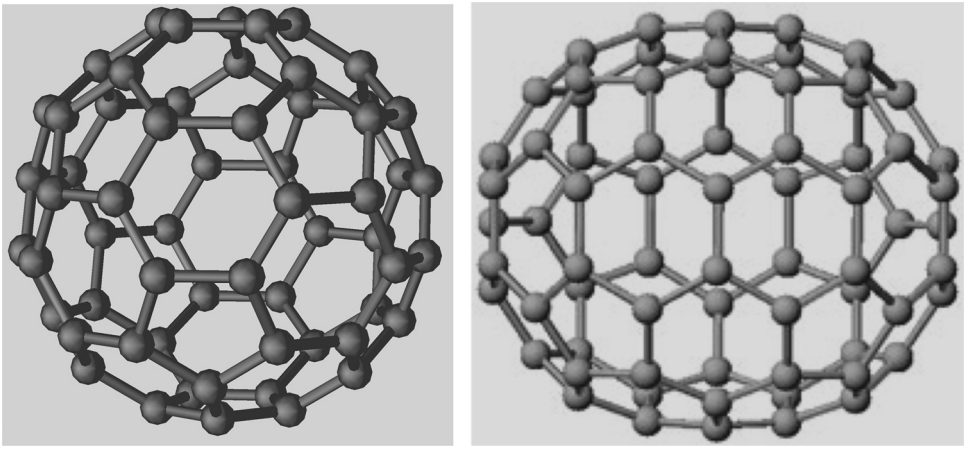

Fig. 1. The structures of C_{60} and C_{70} molecules.

from sheet-like material. These could be used to counteract the considerable discontinuity between the density of gas and of the condensed phase. Later, he suggested that such a cage-shaped molecule could be fashioned out of graphite [60]. He also pointed out that exactly 12 pentagons are required to close a cage comprising only pentagons and hexagons. In 1985, Kroto et al. reported their experimental discovery of a 60-carbon cluster in the mass spectrum of laser-evaporated graphite [1]. Another cluster containing 70 carbon atoms was found to be the next most abundant peak in the mass spectrum. The authors proposed a closed-cage, truncated-icosahedral structure and named the molecule Buckminsterfullerene in honor of R. Buckminster Fuller who introduced geodesic structures in architecture. Fig. 1 shows the structures of C_{60} and C_{70} molecules. They both show closed-cage structures. C_{60} contains 12 pentagons and 20 hexagons of carbon rings, and C_{70} contains 25 hexagons and 12 pentagons.

Krätschmer et al. found an efficient method of synthesizing C_{60} and C_{70} in gram quantities—by arcing graphite electrodes [2]. This gave rise to a burst of studies on these molecules, a renaissance in the study of the properties of fullerenes and carbon in different allotropes [3,4].

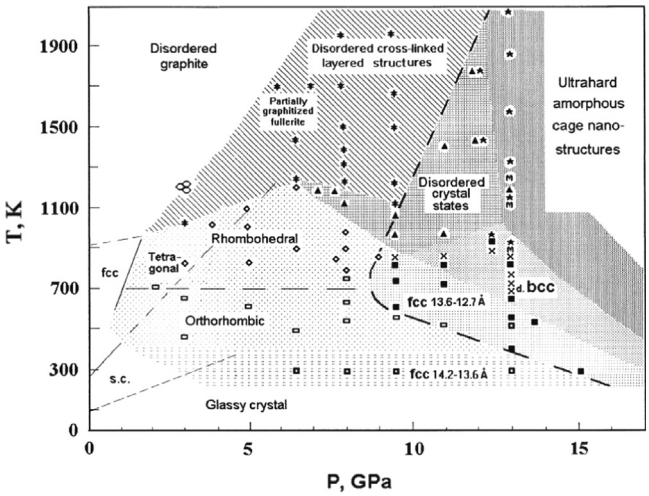

Fig. 2. Phase diagram of C_{60} showing the structural phases obtained under the pressure–temperature conditions shown. (Reprinted with permission from B. Sundqvist [20]).

3. Fullerenes under high pressure

Due to their super-strong covalent intramolecular C–C bonds, C_{60}, the most common fullerene, has been predicted to have an extremely large bulk modulus of around 800–900 GPa for an individual molecule [61,62]. This value is almost twice that of diamond (442 GPa), which is the hardest known material [63]. For this and several other reasons, high-pressure studies of fullerenes have drawn a lot of attentions since the 1990s [58,64–70].

C_{60} molecules form a face-centered cubic (fcc) structure under ambient conditions. Under compression conditions, the crystal undergoes an orientation transition at around 0.4 GPa, causing the fcc structure to transforms into a simple cubic (sc) structure [18,65,71]. The sc structure can persist at a pressure of 25 GPa. At higher pressure, C_{60} cages start to collapse and the crystalline structure becomes amorphous [65,72]. This pressure-induced amorphization is irreversible.

Because the formation of bonds between neighboring C_{60} molecules is a thermally activated process, the polymerization reaction is very slow at room temperature and molecular C_{60} is therefore stable at high pressures and temperatures below ~350–400 K [18–20]. However, many studies have provided evidences suggesting that C_{60} polymerizes at pressure over 4 GPa at room temperature [73,74]. Upon heating at high pressure, C_{60} has a variety of polymerized phases [18–20]. Fig. 2 shows a pressure–temperature phase diagram of C_{60}.

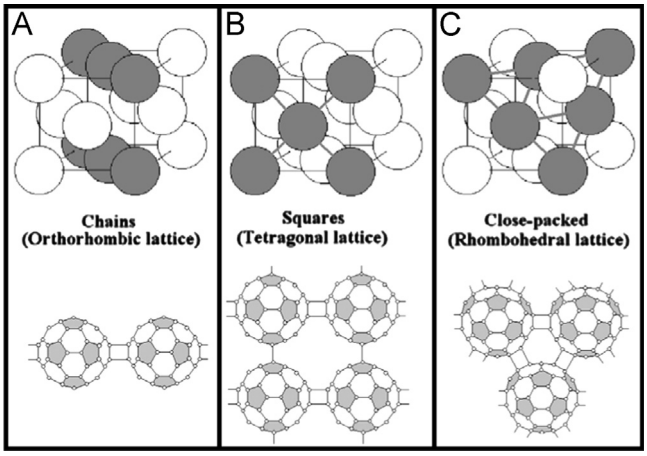

Fig. 3. Basic structures of the three low-dimensional phases of C_{60}. (Reprinted with permission from B. Sundqvist [20]).

Under high-pressure conditions (~1.5 GPa) and at high temperatures (373–473 K), C_{60} dimerizes, when the crystal structure is still in sc [75]. Long linear clusters or chains are believed to form and a phase transition from sc to an orthorhombic phase occurs at higher pressures (~0.7–9 GPa) and temperatures (< 700 K) [76–78]. As shown in Fig. 3A, the chains are along the (1 1 0) direction.

At higher temperatures (> 700 K), the number of intermolecular bonds increases and complete two-dimensional (2D) polymerization phases have been observed at the pressure range of ~1 to ~9 GPa. As shown in Fig. 3B and C, the 2D sheets of linked molecules can form in two ways. One is that the nearest neighbors in the (1 0 0) plane are bound together into squares forming a tetragonal lattice. In another formation the molecules in the close-packed (1 1 1) plane form a trigonal polymer sheet and generate a rhombohedral lattice [18,20]. The new structures are stable at a wide range of pressure–temperature conditions including atmospheric pressure [79].

Three-dimensional (3D) polymerization becomes highly probable at higher pressures (> 8 GPa) upon heating [18,20]. The profile analysis of the diffractions obtained for C_{60} samples quenched from 13 GPa and 670–820 K yielded proof of the formation of 3D polymerized C_{60} phase. From the simulations of possible structures it was concluded that the most probable structure of 3D polymerized C_{60} synthesized at the conditions is a body-centered orthorhombic Immm structure [80,81]. The authors further suggested that the formation of this structure starts with 1D chains by (2+2) cycloaddition, followed by 2D polymerization by four-sided rings. At higher temperatures, further bonds form between 2D layers by a (3+3) cycloaddition reaction resulting in a 3D polymerization C_{60} phase. Marques and coworkers synthesized 3D C_{60} polymer at 13 GPa and 800–820 K, and studied its anisotropic property [82,83]. Interestingly, they found an elliptical Debye-Scherrer pattern due to strong anisotropic pressure effect. It has been reported that 3D C_{60} show interesting mechanical and thermal properties, although the results reported by different groups are still controversial.

Submitting the material to further pressure can cause the structure become random or amorphous and the cages are still intact and form the basic building blocks of the structure [84]. As the pressure increases even further (> 12 GPa) at high temperatures (> 1100 K), the cages start to collapse and form a second amorphous phase containing carbon fragments [85,86]. At temperatures near 2000 K, diamonds can form when at pressures higher than 10 GPa [18–20].

C_{70} is much more complicated and less studied than C_{60}. Unlike C_{60}, which has a pure fcc structure at room temperature, all real C_{70} crystals contain mixtures of several structural phases mainly of fcc and hexagonal closed packed (hcp) structures because of the molecular anisotropy. There are many degrees of freedom. The structure of C_{70} under high-pressure conditions was studied by Wasa et al. using Raman scattering up to 51 GPa at room temperature [87]. A majority of the intramolecular vibrational modes disappeared and only one broad band associated with amorphous carbon was found to persist as pressures above 12 GPa, suggesting an occurrence of pressure-induced amorphization. The transition was shown to be complete by around 18 GPa. The amorphous phase was irreversible at pressures above 35 GPa. Earlier high pressure X-ray diffraction studies of C_{70} nanorods showed pressure-induced amorphization to take place at pressures of ~23 GPa, indicating a strong effect in nanoscale fullerenes crystal [66]. Very recently, C_{70} molecules were found to remain intact at pressures of up to 43 GPa, suggesting an even stronger size effect in fullerenes of smaller size [70].

Like C_{60}, C_{70} polymerizes at elevated temperatures under high-pressure. Fig. 4 shows a pressure–temperature phase diagram of

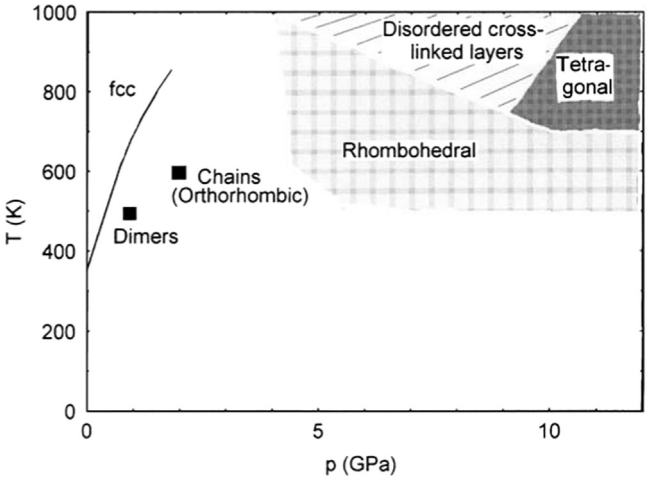

Fig. 4. Pressure–temperature phase diagram of C_{70}. (Reprinted with permission from B. Sundqvist [20]).

C_{70} [18,20]. It is found that the reaction diagram of C_{70} shows some general features with that of C_{60}, but contains much fewer phases. At relatively low pressures, C_{70} dimerizes. Lebedkin and coworkers synthesized C_{70} dimer at 1 GPa and 473 K [88]. At higher pressure (2 GPa) and higher temperature (500–600 K), crystals of C_{70} containing zig-zag chains are formed [89]. As shown in Fig. 4, a rhombohedral, two-dimensional polymeric phase can be formed over a wide range of temperature and pressure. At pressures above 9 GPa tetragonal, three-dimensional polymers are produced [90].

The band structures of fullerenes have been studied under high-pressure conditions. C_{60} is a semiconductor with a band gap of 1.7 eV. It was expected that C_{60} becomes metallic under high pressure. The band gap of C_{60} under high-pressure conditions was measured using optical absorption spectroscopy [72]. The absorption edge shifts to lower energy as pressure increasing. The absorption edge shift was reported to be −0.05 eV/GPa by Moshary et al., suggesting that metallization could occur by 33 GPa [72]. However, the molecules collapse at pressures of 25 GPa and render metallization of pure fullerite inaccessible. The resistivity of fullerenes under high pressure has also been measured by several other research groups. No metallization has been found. The resistivity was found to increase during the amorphization transition of C_{60} [68].

4. Solvated fullerenes

Fullerenes are soluble in small amounts in many solvents including aromatics, such as toluene, xylene, and benzene, and others such as carbon disulfide. The solubility of fullerenes in many solvents has been determined. Table 1 shows solubility of C_{60} and C_{70} in some solvents. Their solubility varies significantly in different solvents [91].

The solubility of fullerenes shows an unusual behavior in many solvents due to the relatively strong interactions between fullerenes and solvents, which causes the formation of solvate phases [92]. For example, C_{60} shows maximum solubility in benzene at about 313 K. Crystallization from benzene solution at temperatures below maximum results in formation of triclinic solid solvate with four benzene molecules $C_{60}\cdot 4C_6H_6$ which is unstable in air [35,36,45]. The preparation and characterization of solvated fullerenes have been widely studied [26–45]. Many fullerene solvates have been observed and make this group of materials an important class of fullerenes. In this section, the research status of fullerenes solvates is briefly reviewed.

Table 1
The solubility of C_{60} and C_{70} in some solvents. [91].

Solvent	C_{60}	C_{70}
1-Chloronaphthalene	51 mg/mL	
1-Methylnaphthalene	33 mg/mL	
1,2-Dichlorobenzene	24 mg/mL	36.2 mg/mL
1,2,4-Trimethylbenzene	18 mg/mL	
Tetrahydronaphthalene	16 mg/mL	
Carbon disulfide	8 mg/mL	9.875 mg/mL
1,2,3-Tribromopropane	8 mg/mL	
Chlorobenzene	7 mg/mL	
Xylene	5 mg/mL	3.985 mg/mL(*p*-xylene)
Cumene	4 mg/mL	
Toluene	3 mg/mL	1.406 mg/mL
Benzene	1.5 mg/mL	1.3 mg/mL
Carbon tetrachloride	0.447 mg/mL	0.121 mg/mL
Chloroform	0.25 mg/mL	
n-Hexane	0.046 mg/mL	0.013 mg/mL
Acetonitrile	0.004 mg/mL	
Methanol	0.00004 mg/mL	
Pentane	0.004 mg/mL	0.002 mg/mL
Heptane		0.047 mg/mL
Octane	0.025 mg/mL	0.042 mg/mL
Decane	0.070 mg/mL	0.053 mg/mL
Dodecane	0.091 mg/mL	0.098 mg/mL
Acetone		0.0019 mg/mL
Isopropanol		0.0021 mg/mL
Dioxane	0.0041 mg/mL	
Mesitylene	0.997 mg/mL	1.472 mg/mL
Dichloromethane	0.254 mg/mL	0.080 mg/mL

4.1. Preparations of solvated fullerenes

C_{60} and C_{70} fullerenes form solvates with almost all common solvents. Reported data for most of these solvates are summarized in Table 2. It can be seen that solvated fullerenes have been synthesized using a variety of solvents, including pentane [37], hexane [38], heptane [39], benzene [34–36], and CS_2 [40,41], 1,1,2-trichloroethane (CH_3CCl_3) [27]. In general solvated fullerenes can be synthesized by evaporating fullerene solutions. The earliest study on solvated fullerenes can be traced back to early 1990s. The solvate of C_{60} was realized soon after the report of large quantity synthesis of C_{60} using contact-arc vaporization of a graphite rod during extraction process [93]. The first report focused on solvated C_{60} and C_{70} was probably published by Fleming et al. in July, 1991 [26]. Pentane-solvated C_{60} and C_{70} were studied. The crystals appeared long and in ten-sided columns. Single crystal X-ray diffraction was performed. Results indicated that the crystals appeared in crystalline order with a twinned unit cell. In November 1991, Gorun et al. prepared cyclohexane-solvated C_{60} and C_{70} using slow cooling of supersaturated solutions of C_{60} and C_{70} mixtures for their structure studies [42]. However, solvates were found to lose their crystallinity when exposed to air because of solvent loss. Slow evaporation of benzene solution of C_{60} at around temperature of 50°C can produce benzene-solvated C_{60}. The stoichiometric ratio of C_{60} to solvent was determined to be 1:4. From 1996–2007, the research group led by Tamarit has made considerable contributions to this field [27,32,33,38,97,98]. Several fullerene solvates were synthesized and systematically characterized using X-ray diffraction (XRD), thermogravimetry (TGA), and differential scanning calorimetry (DSC). Aging studies of different solvates in the time scale of years were also performed. Korobov et al. studied the structures of 12 solvates (Table 2) of C_{60} and C_{70} with different structures and stoichiometry using XRD to establish a relationship between the X-ray and the thermodynamic data on solvated fullerene solvated crystals [94]. Solvates were found to be typical van-der-Waals complexes with negative excess volumes with packing coefficients from 0.72 to 0.78. These are stable due to the formation of the bonds between fullerenes and solvent.

In synthesis, temperature plays an important role in the formation of solvated fullerenes. It affects stability and stoichiometry. For instance, C_{60}∗*m*-xylene remains stable at temperatures of up to 333 K [28,29]. However, C_{60}∗toluene only remains stables at low temperatures (150 K) [45]. For *m*-$C_6H_4Br_2$-solvated C_{60}, the stoichiometric ratio changes at different temperatures. C_{60}∗2*m*-$C_6H_4Br_2$ is only stable at low temperatures, and C_{60}∗2/3*m*-$C_6H_4Br_2$ can be stable at room temperatures [94].

The incorporation of guest molecules into the host C_{60} lattice changes its crystal structure. As shown in Table 2, there are at least five types of packing symmetry relevant to these materials. They include hexagonal, cubic, monoclinic, triclinic, and orthorhombic. The structure is dependent on both the solvent and stoichiometric ratio. For example, C_{60} crystals grown in cyclohexane crystallize in the cubic system [42], C_{60} crystals with CS_2 or *n*-pentane have orthorhombic structures [41], and C_{60} solvates grown from benzene and *n*-heptane have a hexagonal lattice [31]. C_{60}∗2$BrCCl_3$ has a hexagonal lattice, however C_{60}∗12$BrCCl_3$ is in cubic [99]. The solvents with symmetrical geometry and small size should be able to fit in the large octahedral voids of fullerene lattices and cause no change of the crystal structure. For example, C_8H_8, a cubic molecule, occupies the interstitial octahedral sites of C_{60} and forms C_{60}∗C_8H_8 with an fcc structure which is same as for the pure C_{60} crystals. When solvents have non-symmetric geometry or polar molecules, the solvated fullerenes cannot stay in their mother structure in most of cases. The species of solvent and crystal structure can highly affect their high pressure polymerization behavior.

Solvate crystals of different shapes form from different solvents. Taking 1,1,2-trichloroethane and bromotrichloromethane ($BrCCl_3$) as examples, the C_{60} 1:1 solvate formed with 1,1,2-trichloroethane showed a needlelike shape with a polyhedral cross section, but C_{60}∗2$BrCCl_3$ showed interpenetrating hexagonal single crystals, indicating that the polymorphism of C_{60} is solvent-dependent [32]. Another interesting example is *m*-xylene, which was used as a shape controller in synthesis of nanorods of C_{60}. Single-crystalline C_{60}∗1*m*-xylene nanorods with a hexagonal structures were successfully synthesized by evaporating a C_{60} solution in *m*-xylene at room temperature. The hexagonal structures change into cubic structures due to total loss of solvent at temperature over 333 K. They produce pure C_{60} nanorods. The ratio of the length to the diameter of the nanorods can be controlled within a range of 10 to over 1000 for different applications. Fig. 5 shows a SEM picture of as-grown C_{60}∗1*m*-xylene solvate nanorods. No changes in shape were observed during heating events, which involved loss of solvent [28,29].

4.2. Physical properties of solvated fullerenes

The properties of solvated fullerenes have also been studied. Guest molecules were also found to change the vibrational properties of the fullerene crystals and thus the Raman and IR (infrared absorption) spectra of C_{60}. The Raman spectra of C_{60} solvates formed in solvents such as benzene and toluene showed new peaks not visible in the spectra of pristine C_{60}, and other peaks shifted location [31]. Graja et al. reported that the guest molecules can hinder the rotation of C_{60} molecules which leads to a decrease of vibrational–rotational couplings [44,45]. However, the NMR measurements on C_{60}∗4benzene suggest that interactions between benzene and C_{60} molecules are very weak, and the rotation of C_{60} is not hindered [35,106]. It is therefore very interesting to study the solvent-dependent polymorphism and the properties of C_{60} solvates formed with various solvents.

Table 2
Summary of information of most of reported fullerenes solvates.

	Crystal structure	Stability in air at ambient (T)	Characterization technique used	Refs.
C_{60}*1*m*-xylene	Hcp, a=2.376 nm, c=1.008 nm	Stable	XRD, Raman, IR, TGA, TEM, SEM	[28]
C_{60}*4C_6H_6	hcp		XRD, Raman	[31,34,45,94]
C_{60}*10CCl_4	Fcc a=2.739 nm	Stable	XRD	[95]
C_{60}*$C_6H_5CH_3$	Monoclinic	Metastable	IR, Raman	[31,45]
C_{60}*0.5 $C_6H_5CH_3$			IR	
C_{60}*decalin	hcp		IR	
C_{60}*6*n*-decane (210 °C)			IR	
C_{60}*3*n*-decane (340 °C)			IR	
Cf_{60}*2$CHBr_3$	Hcp, a=1.0226 nm, c=1.0207 nm		XRD, TGA, NMR	[96]
C_{60}*1,1,2-trichloroethane	Orthorhombic a=1.0164 nm b=3.1390 nm c=1.0130 nm	Metastable	SEM, XRD, TGA	[27]
C_{60}**n*-hexane	Orthorhombic a=1.0249 nm b=3.1308 nm c=1.0164 nm	Stable	XRD, TGA, Raman	[31,38]
C_{60}*H_2CCl_2	Cubic A=2.3284 nm	Unstable	XRD, TGA	[97]
C_{60}*2Ferrocene	Triclinic			[98]
C_{60}*12$BrCCl_3$	Cubic A=2.7591 nm	Unstable	XRD, TGA, SEM	[99]
C_{60}*2$BrCCl_3$	Hexagonal a=1.016 nm b=1.089 nm	Stable		
C_{60}*2/3*n*-nonane	Orthorhombic a=1.010 nm b=1.019 nm c=4.871 nm	Stable	SEM, XRD, TGA	[100]
C_{60}*2$(CH_3)CCl_3$	Monoclinic			[33]
C_{60}*2$C_6H_5CH_3$	Monoclinic		XRD, Differential scanning calorimetry (DSC)	[94]
C_{60}* $C_6H_5CH_3$	Monoclinic			
C_{60}*2C_6H_5I	Monoclinic			
C_{60}*3*m*-$C_6H_4Br_2$	Monoclinic			
C_{60}*2*m*-$C_6H_4Br_2$	Monoclinic			
C_{60}*C_6H_5Cl	Monoclinic			
C_{60}*2*o*-xylene	Monoclinic			
C_{60}*2/3*m*-$C_6H_4Br_2$	Hexagonal			
C_{60}*2/3*m*-xylene	Hexagonal			
C_{60}*2/3*m*-$C_6H_4Cl_2$	Hexagonal			
C_{60}*2/3$C_6H_3(CH_3)_3$	Hexagonal			
C_{70}*2*o*-xylene	Triclinic			
C_{70}* Ferrocene	Monoclinic a=2.938 nm b=1.036 nm c=2.021 nm			[101]
C_{70}*2mesitylene	Cubic a=1.04774 nm	Stable	XRD, TGA, SEM, Fluorescence	[102]
C_{60}*CS_2	Monoclinic		NMR	[40,41]
C_{60}*C_8H_8	Fcc a=1.474 nm	Stable	XRD, TEM, Raman, IR, TGA, and Mass spectrometry, NMR	[103]
C_{70}*C_8H_8	Tetragonal (room temperature) *I*4/*mmm* FCC (at > 375 K)	Stable	XRD, TEM, Raman, IR, TGA, and Mass spectrometry, NMR	[103,104]
C_{60}*S_{16}	Monoclinic a=20.867(4) Å, b=21.062(4) Å, c=10.508(2) Å, β=111.25(7)°	Stable	XRD, Raman	[105]
C_{60}**n*-pentane	Orthorhombic		XRD	[37]
C_{60}*heptane	Hexagonal a=1.000(4) nm b=1.016(1) nm	Stable	XRD, TGA, SEM	[39]
C_{60}*TDAE	Monoclinic a=1.5849 nm b=1.2987 nm c=0.9965 nm β=93.31°	Unstable	XRD, magnetic measurement, electron spin resonance	[55]

In solvated C_{60}, the orientational ordering transition was found to be smeared and shifted to lower temperatures. For example, the orientational transition shifted to 170 K in C_{60}:*n*-hpentane and below 77 K in C_{60}:CS_2 [37,41,45].

The interactions between fullerenes and solvents reduce the icosahedral symmetry of fullerene molecules, making electronic transitions previously impossible in pristine fullerenes possible. This changes their optical properties. The photoluminescence (PL)

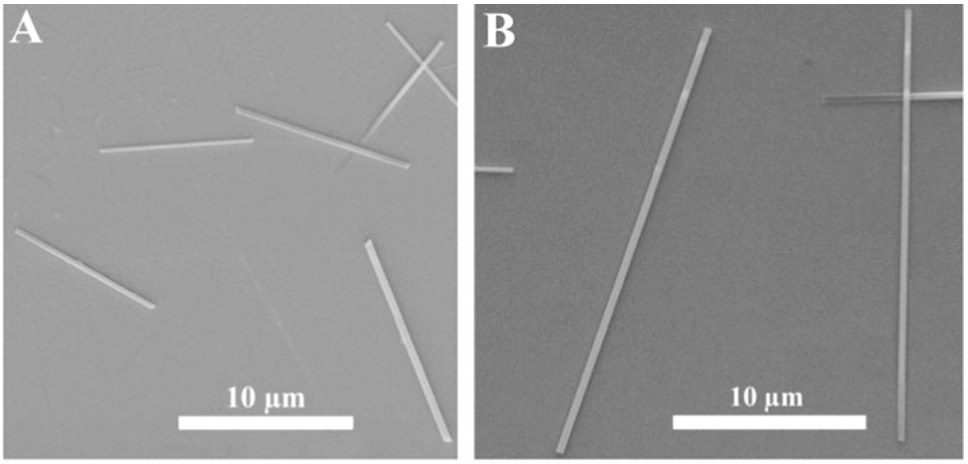

Fig. 5. SEM images of as-grown C_{60}*1*m*-xylene solvate nanorods. [28,29] (Reprinted with permission from Wang et al. [29]).

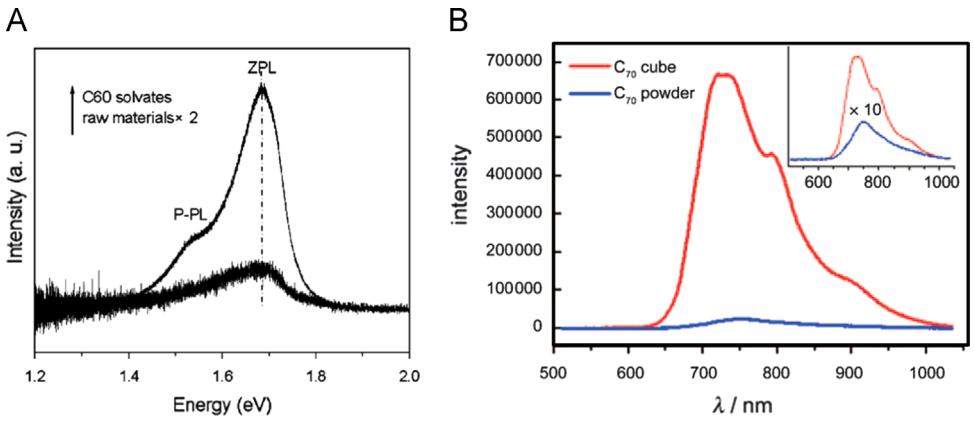

Fig. 6. PL spectra of C_{60}*m*-xylene solvate and pristine C_{60} (A), and C_{70}*2mesitylene solvate and pristine C_{70} powder (B). (Adapted from [28] and [102]).

of C_{60}*m*-xylene was studied by the present team. The PL intensity of the solvate was found to be about 2 orders of magnitude higher than those of pristine C_{60}, as shown in Fig. 6. The quantum yield of the solvate was found 1 to 2 orders of magnitude higher than C_{60} as well. The extra Raman peaks observed in the solvate suggest van-der-Waals interactions between the C_{60} molecules and the solvents, which reduces the symmetry of the C_{60} molecular and renders electric-dipole transitions that were impossible with pristine C_{60} due to high symmetry possible [28]. This phenomenon has also been observed in C_{70} solvates [102].

5. High-pressure studies of solvated fullerenes

The high-pressure study of solvated fullerenes has attracted a lot of attentions. Several solvates of C_{60} and C_{70} with different solvent and structures have been systematically studied using techniques including XRD, Raman spectroscopy, inelastic X-ray scattering (IXS) spectroscopy, infrared absorption (IR) spectroscopy, high-resolution transmission electron microscopy (HRTEM), and theoretical calculations. Several new phenomena have been observed [46,107–109]. In this section, all recent studies and results will be briefly reviewed.

C_{60}*TDAE is an organic ferromagnetic material with high Curie temperature of 16.1 K. Effects of hydrostatic pressure on C_{60}*TDAE were investigated by electron spin resonance to reveal a mechanism of the ferromagnetism. It was found that the transition temperature Tc decreases with increasing pressure, reaching zero around 0.9 GPa. Fig. 7 shows the pressure dependence of Tc. Above

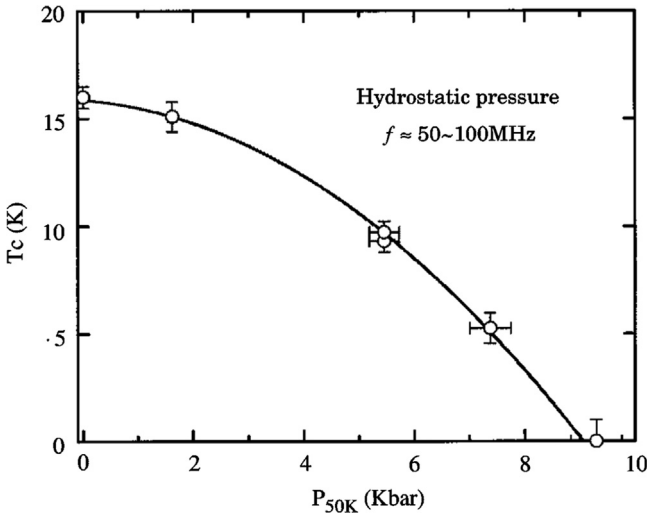

Fig. 7. Tc versus P50 K in C_{60}*TDAE. The solid curve indicates the theoretical predition with the data up to 7.4 kbar. (Reprinted with permission from Mizoguchi et al. [56]).

about 1 GPa at 300 K, it was found to transform to the one-dimensional polymerized phase. The new phase is stable even after pressure release [55–57]. The effects of uniaxial strain on Tc of C_{60}*TDAE single crystal were also studied. Tc as functions of pressure applied along *b*- and *c*-axis together with hydrostatic pressure is shown in Fig. 8. It is clear that magnetic

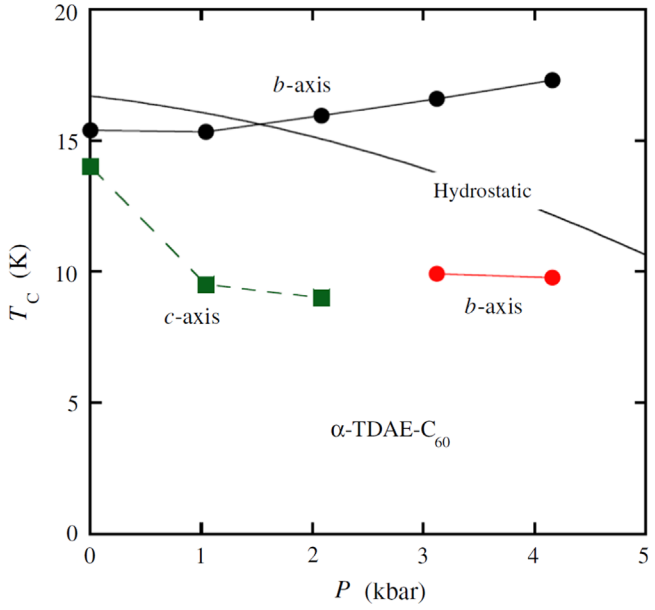

Fig. 8. Tc variations caused by uniaxial strain along *b*-axis [110] and *c*-axis, together with by hydrostatic pressure [111] (Reprinted with permission from Mizoguchi et al. [57]).

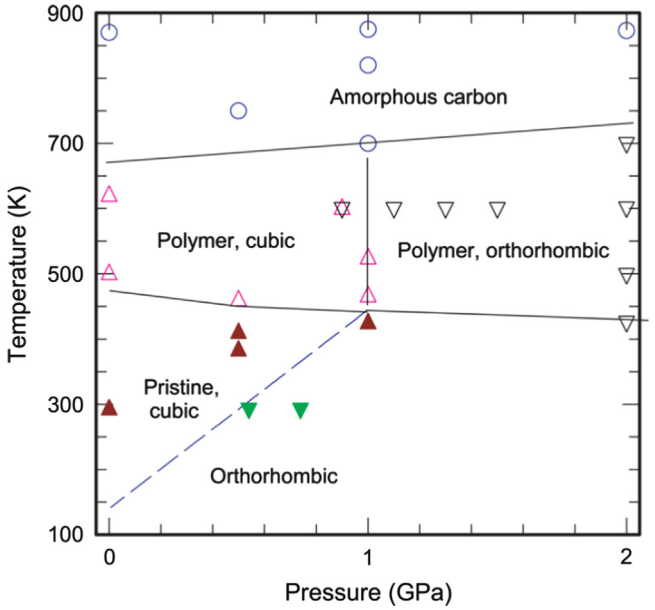

Fig. 9. Pressure–temperature phase diagram of C_{60}*C_8H_8. (Reprinted with permission from Iwasiewicz-Wabnig et al. [47]).

interactions are anisotropic. The *b*-axis strain enhances Tc up to 17.5 K under 4 kbar of the applied pressure. The *c*-axis strain strongly suppresses the ferromagnetism. It is interesting that the *b*-axis strain also produces a fraction of the sample with the low Tc of about 10 K [57].

The rotor-stator compound C_{60}*C_8H_8 was studied up to 10 GPa at room temperature using infrared transmission [46–51]. It was found that kinks appeared in the pressure dependences of the frequencies of the molecular vibrations at around 0.8 GPa, suggesting the occurrence of an orientational ordering transition at room temperature. The qualitative features of the spectra at high pressure indicate a symmetry lowering of the fullerene molecules. The higher transition pressure in C_{60}*C_8H_8 compared to C_{60} could be attributed to the expanded lattice. The cubane vibrational modes survive up to a higher pressure compared to the C_{60} modes, suggesting a considerable shielding of C_8H_8 molecules from pressure in the interball voids in the crystal. The pressure–temperature phase diagram of C_{60}*C_8H_8 was systematically studied by Iwasiewicz-Wabnig et al. [46,47]. They annealed C_{60}*C_8H_8 at different temperatures in the range of 380–870 K under pressures up to 2 GPa. The treated samples were then investigated under ambient conditions using Raman spectroscopy and X-ray diffraction. C_{60}*C_8H_8 was found to have at least five different phases depending on the treatment conditions, as shown in Fig. 9 [47]. The pressure–temperature phase diagram is different from that of pure C_{60} suggesting the effect of C_8H_8 molecules.

$C_{60}S_{16}$ is made of C_{60} and S_8 rings. Talyzin et al. studied high pressure Raman of this material up to 12.4 GPa [52]. It was found that C_{60} molecules in this compound polymerize similar to the pure C_{60}. However, the vibration peaks in the Raman spectra are much sharper, suggesting better ordering of C_{60} polymerization within $C_{60}S_{16}$. It was explained that such ordering is achieved because of the layered structure of the $C_{60}S_{16}$ where the sulfur rings prevent polymerization in the *c*-axis of monoclinic lattice. The peaks from S_8 rings disappeared and new peaks were observed at higher pressures. These changes suggested the sulfur rings are broken and covalent C–S bonds may be formed. The Raman spectrum of quenched sample shows some similarities to that of $C_{60}O$ suggesting that at least part of the sample consists of $C_{60}S$ [52].

Meletov and Konarev recently studied pressure-induced charge transfer transition in the donor-acceptor complexes C_{60}{Ni($nPr_2dtc)_2$} and C_{60}{Cu($nPr_2dtc)_2$} using Raman spectrograph up to 7 GPa at room temperature [53]. It was found the Ag(2) mode of C_{60} split at about 0.7 GPa. The peak showed an overall softening by $\sim$6 cm^{-1} near 2 GPa, while the pressure dependence is reversible with some hysteresis. The authors believe that the observed peculiarities are associated with the pressure-induced charge transfer of one electron from the organic donor to the fullerene acceptor. Pressure-induced phase transitions in another molecular donor-acceptor complex C_{60}{Pt(dbdtc)$_2$} (C_{60} fullerene with platinum dibenzyldithiocarbamate) were also investigated by the same group up to 8 GPa [54]. It was found that the vibration modes related to the C_{60} split and soften in the low pressure regime ($P < 0.5$ GPa), indicating the formation of intercage covalent bonds. At the pressure of $\sim$2.5 GPa, additional splitting of Raman modes was observed and was attributed to the formation of a polymeric network. The high pressure phase remains stable upon pressure decrease, however the material transforms into a new phase which is different from those of the known polymerized C_{60} at 0.5 GPa.

The high-pressure study of *m*-xylene solvated C_{60} up to 60 GPa was studied using a diamond anvil cell by Wang et al. [58]. The crystal structure, lattice vibration, and bonding type of the material at high pressures were analyzed experimentally. Surprisingly, there was found to be no drastic changes other than gradual shifts, broadening, and weakening of diffraction peaks. The presence of diffraction peaks at the highest pressures indicates that the long-range periodicity of the molecules remains intact. This is in contrast with pristine pure C_{60}, where the face-centered cubic periodicity of C_{60} molecular units disappears when it amorphizes above 30 GPa. The Raman spectra of the materials recovered from procedures performed at different pressures suggest that C_{60} cages start to collapse at around 32 GPa and completely transform into amorphous carbon clusters at higher pressures. But, the XRD of the samples recovered from 35 and 42 GPa show clear diffraction peaks of hcp lattice. All these suggest that even C_{60} cages completely collapse and transform into amorphous clusters at pressures higher than 32 GPa. The overall hcp lattice is preserved, forming ordered amorphous carbon clusters (OACC). Fig. 10 shows the simulated structures of the materials at different pressures and

upon decompression. In-situ high pressure IXS studies suggest the bonding transition of sp2 to sp3 during the collapse of C_{60} at high pressures. To confirm the important role of solvent, a heating treatment was performed for the material recovered from 40 GPa to remove solvent. The treated sample was then studied by XRD. The pattern shows a typical amorphous feature, suggesting that the material loses its long-range periodicity after the solvent is evaporated. This confirms the critical role of the solvent in maintaining long-range periodicity. For practical applications, it is more important that the OACC is quenchable and as incompressible as diamond. Fig. 11 shows the optical pictures of the ring cracks in the diamond anvils generated after formation of OACC and then release of the pressure.

Solid-state materials can be categorized by their structures into crystalline (with periodic translation symmetry), amorphous (without periodic or orientational symmetry), and quasi-crystalline (with orientational but not periodic translation symmetry). This study discovered the first crystalline material made with amorphous building blocks.

After this discovery, Yao et al. studied the behavior of C_{60}*m*-xylene solvate and the desolvated C_{60} using in-situ Raman spectroscopy [107]. The formation of the OACC at high pressure was further confirmed. In the experiments, the structural transformation of solvated and desolvated C_{60} molecules was found to be similar, both undergoing deformation and amorphization at high pressures. However the mechanical properties of the high-pressure phases are significantly different. The high-pressure phase of the solvated sample created clear ring cracks on the diamond anvils, as shown in these experiments at different pressures, confirming previous results. In contrast the desolvated sample created only a very small crack in one experiment, and it is noted that no cracks were produced in another experiment. These suggest that the transformations of the two materials are different due to the presence of solvent. The creation of OACC at high pressures was confirmed directly by HRTEM measurements on decompressed sample. The selected area electron diffraction of OACC can be indexed in a hexagonal structure, which is in constant with our previous XRD result. HRTEM showed the desolvated sample from 44.5 GPa to contain amorphous phase and a small amount of ordered phase. The results indicate that the solvent plays a crucial role in keeping long-range periodicity in the released solvated materials, as concluded in a previous report.

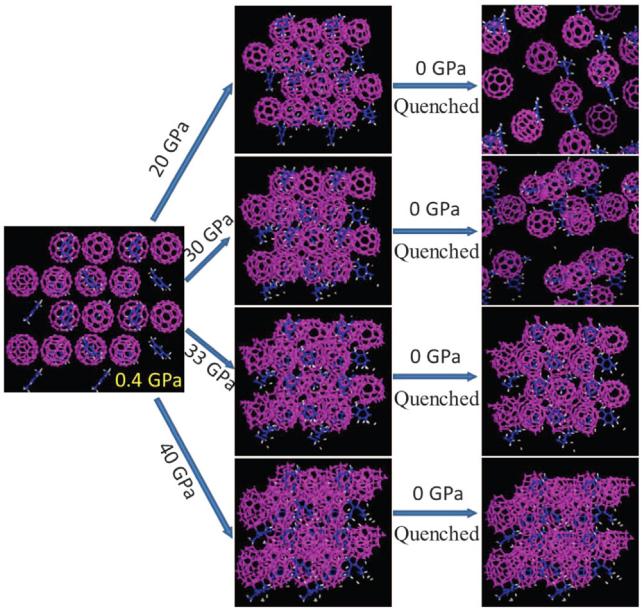

Fig. 10. Simulated structures of the material under different compression and decompression conditions. (Reprinted with permission from Wang et al. [58]).

Using Raman spectroscopy, Cui et al. studied high-pressure polymerization of $C_{60}(Fe(C_5H_5)_2)_2$ ($C_{60}(Fc)_2$) and found a reversible polymerization. In-situ high-pressure Raman studies were carried out on single crystalline $C_{60}(Fc)_2$ molecules at pressures of up to 25.4 GPa [108]. The Raman results show that the charge transfer between Fc (ferrocene) and C_{60} increases in the low-pressure range. At pressures above 5 GPa, C_{60} molecules start to form a chainlike polymer structure. However, this polymerization is reversible upon decompression, unlike that of pristine C_{60}. From a structural perspective, the layered structure of $C_{60}(Fc)_2$ restricts the polymerization of C_{60} molecules in some directions. This explains why only linear chainlike polymeric structures of the C_{60} lattice form under pressure. It has also been suggested that the reversible polymerization is related to the increased charge transfer and the overridden steric repulsion of counterions.

Similarly, Cui et al. found a reversible pressure-induced polymerization of Fc solvated C_{70} [109]. High-pressure Raman spectroscopy, IR, and XRD were carried out on this solvated fullerene. Theoretical calculations were used to analyze the electron localization function and charge transfer in the crystal to facilitate understanding of the transformation under high-pressure conditions. The results showed that even dimeric and one-dimensional polymeric phases can be formed at about 3 and 8 GPa at room temperature. The polymerization was found to be reversible upon decompression. The reversibility of the polymerization may be related to pressure-tuned transfers of charge and the overridden

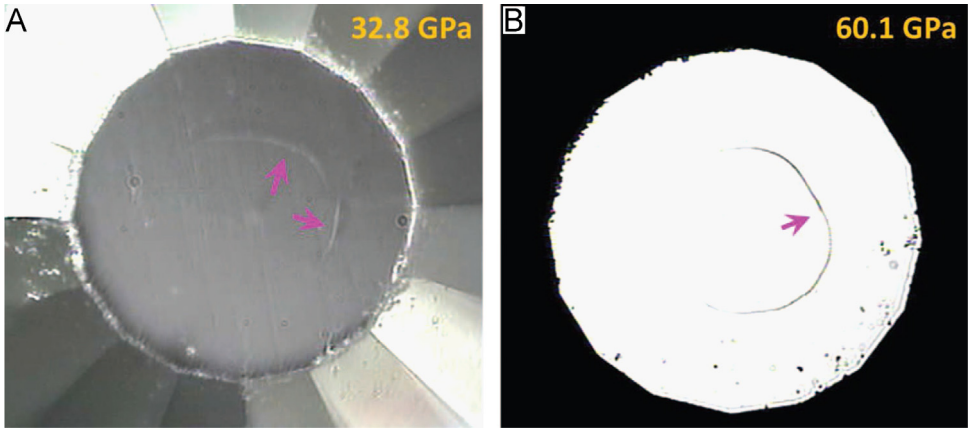

Fig. 11. Optical pictures of the ring cracks in the diamond anvils generated after formation of OACC and then release of the pressures from 32.8 GPa (A), and 60.1 GPa (B). (Reprinted with permission from Wang et al. [58]).

steric repulsion of counterions, similar to that reported for $C_{60}(Fc)_2$. Fc solvated C_{70} was also found to have a layered structure of the intercalated ferrocene molecules formed in the crystal. This suggests that ferrocene acts not only as a spacer to restrict the polymerization of C_{70} molecules within a layer but also as a charge reservoir to tune the polymerization process.

Very recently, the high-pressure behavior of fullerene solvates that form orthorhombic and cubic structures was studied by us. High-pressure behaviors, including phase transformation and polymerization, were not only solvent-dependent but also symmetry-dependent.

As discussed above, the structure of solvated fullerenes is solvent-dependent and an extensive class of crystalline-solvated fullerenes can be obtained by changing the solvent species and the ratio of fullerenes to solvent. This suggests that the study of solvated fullerenes under high-pressure conditions is only beginning. More investigations are needed, and more phenomena and new discoveries can be expected.

6. Summary and future prospects

Studies of solvated fullerenes at high pressure have made a lot of progresses. Because this area of research is just at its beginning, there is a lot of potential yet to be exploited. In particular, phase transition, equation of state, and stability of materials are fundamental questions in physics and material science. The studies shown here indicate that solvents have big impact on the properties of these solvates. However, most of the solvates have not yet been studied and not all of the properties of the solvated materials are known yet. In this way, systematic, high-pressure studies of the solvates are expected. Pristine C_{60} is a semiconductor. However, the electronic properties of solvated fullerenes and their high pressure phases are still unknown. More experimental and theoretical investigations are expected in near future.

Polymerization of pristine fullerenes under high pressure conditions has become an important topic and many discoveries have been made during the past 20 years. The pressure-induced polymerization of solvated fullerenes is very different from that of pure fullerenes because of the presence of solvent. More systematic studies are also expected in this direction. All these may deepen our understanding of fullerenes and condensed matter.

Acknowledgements

Acknowledgments: This work was supported as part of EFree, an Energy Frontier Research Center funded by the U.S. Department of Energy (DOE), Office of Science under DE-SC0001057. The work was also supported by the National Natural Science Foundation of China (NSFC, 11004072) and Program for New Century Excellent Talents in University (NCET-10-0444).

References

[1] H.W. Kroto, J.R. Heath, S.C. O'Brien, R.F. Curland, R.E. Smalley, C-60 – Buckminsterfullerene, Nature 318 (1985) 162–163.
[2] W. Krätschmer, L.D. Lamb, K. Fostiropoulos, D.R. Huffman, Solid C-60—a new form of carbon, Nature 347 (1990) 354–358.
[3] S. Iijima, Helical microtubules of graphitic carbon, Nature 354 (1991) 56–58.
[4] K.S. Novoselov, A.K. Geim, S.V. Morozov, D. Jiang, Y. Zhang, S.V. Dubonos, I.V. Grigorieva, A.A. Firsov, Electric field effect in atomically thin carbon films, Science 306 (2004) 666–669.
[5] C.N.R. Rao, R.a.m. Seshadri, A. Govindaraj, Rahul Sen, Fullerenes, nanotubes, onions and related carbon structures, Mater. Sci. Eng., R 15 (1995) 209–262.
[6] R.E. Smalley, Self-assembly of the fullerenes, Acc. Chem. Res. 25 (1992) 98–105.
[7] X. Lu, Z.F. Chen, Curved Pi-conjugation aromaticity, and the related chemistry of small fullerenes ($< C_{60}$) and single-walled carbon nanotubes, Chem. Rev. 105 (2005) 3643–3696.
[8] F. Diederich, R.L. Whetten, Beyond C_{60}: the higher fullerenes, Acc. Chem. Res. 25 (1992) 119–126.
[9] R.C. Haddon, Electronic structure, conductivity, and superconductivity of alkali metal doped C_{60}, Acc. Chem. Res. 25 (1992) 127–133.
[10] Y.F. Zhao, Y.H. Kim, A.C. Dillon, M.J. Heben, S.B. Zhang, Hydrogen storage in novel organometallic buckyballs, Phys. Rev. Lett. 94 (2005) 155504.
[11] J.L. Segura, N. Martin, D.M. Guldi, Materials for organic solar cells: the C_{60}/pi-conjugated oligomer approach, Chem. Soc. Rev. 34 (2005) 31–47.
[12] B.C. Thompson, J.M.J. Frechet, Polymer-fullerene composite solar cells, Angew. Chem. Int. Ed. 47 (2008) 58–77.
[13] G.J. Zhang, Y.J. He, Y.F. Li, 6.5% efficiency of polymer solar cells based on poly (3-hexylthiophene) and indene-C-60 bisadduct by device optimization, Adv. Mater. 22 (2010) 4355–4358.
[14] H.K. Mao, R.J. Hemley, Ultrahigh-pressure transitions in solid hydrogen, Rev. Mod. Phys. 66 (1994) 671–692.
[15] R.J. Hemley, A.P. Jephcoat, H.K. Mao, L.C. Ming, M.H. Manghnani, Pressure-induced amorphization of crystalline silica, Nature 334 (1988) 52–54.
[16] L. Wang, W. Yang, Y. Ding, Y. Ren, S. Xiao, B. Liu, S. Sinogeikin, Y. Meng, D.J. Gosztola, G. Shen, R. Hemley, W. Mao, H.-k. Mao, Size-dependent amorphization of nanoscale Y_2O_3 at high pressure, Phys. Rev. Lett. 105 (2010) 095701.
[17] L. Wang, Y. Ding, W. Yang, W. Liu, Z. Cai, J. Kung, J. Shu, R.J. Hemley, W. Mao, H.-k. Mao, Nanoprobe measurements of materials at megabar pressures, Proc. Nat. Acad. Sci. 107 (2010) 6140–6145.
[18] B. Sundqvist, Fullerenes under high pressure, Adv. Phys. 48 (1999) 1–134.
[19] V.D. Blank, S.G. Buga, G.A. Dubitsky, N.R. Serebryanaya, M.Y.u. Popov, B. Sundqvist, High-pressure polymerized phases of C_{60}, Carbon 36 (1998) 319–343.
[20] B. Sundqvist, Polymeric fullerene phases formed under pressure, Struct. Bond. 109 (2004) 85–126.
[21] F. Giacalone, N. Martin, Fullerene Polymers: synthesis and properties, Chem. Rev. 106 (2006) 5136–5190.
[22] E. Burgos, E. Halac, R. Weht, H. Bonadeo, E. Artacho, P. Ordejon, New superhard phases for three-dimensional C_{60} based fullerites, Phys. Rev. Lett. 85 (2000) 2328–2331.
[23] A.F. Hebard, M.J. Rosseinsky, R.C. Haddon, D.W. Murphy, S.H. Glarum, T.T.M. Palstra, A.P. Ramirez, A.R. Kortan, Superconductivity at 18 K in potassium-doped C_{60}, Nature 350 (1991) 600–601.
[24] P.W. Stephens, L. Mihaly, P.L. Lee, R.L. Whetten, S.M. Huang, R. Kaner, F. Deiderich, K. Holczer, Structure of single-phase superconducting K_3C_{60}, Nature 351 (1991) 632–634.
[25] R.M. Fleming, A.P. Ramirez, M.J. Rosseinsky, D.W. Murphy, R.C. Haddon, S.M. Zahurak, A.V. Makhija, Relation of structure and superconducting transition- temperatures in A_3C_{60}, Nature 352 (1991) 787–788.
[26] R.M. Fleming, A.R. Kortan, B. Hessen, T. Siegrist, F.A. Thiel, P. Marsh, R.C. Haddon, R. Tycko, G. Dabbagh, M.L. Kaplan, A.M. Mujsce, Pseudotenfold symmetry in pentane-solvated C_{60} and C_{70}, Phys. Rev. B: Condens. Matter 44 (1991) 888–891.
[27] F. Michaud, M. Barrio, D.O. Lo´pez, J. Ll., V. Tamarit, S. Agafonov, H. Toscani, R. Szwarc, Ce´olin, Solid-state studies on a C_{60} solvate grown from 1,1,2-trichloroethane, Chem. Mater. 12 (2000) 3595–3602.
[28] L. Wang, B.B. Liu, S.D. Yu, M.G. Yao, D.D. Liu, Y.Y. Hou, T. Cui, G.T. Zou, B. Sundqvist, Highly enhanced luminescence from single-crystalline C_{60}*1m-xylene nanorods, Chem. Mater. 18 (2006) 4190.
[29] L. Wang, B.B. Liu, D.D. Liu, M.G. Yao, Y.Y. Hou, S.D. Yu, T. Cui, D.M. Li, G.T. Zou, A. Iwasiewicz, B. Sundqvist, Synthesis of thin, rectangular C_{60} nanorods using *m*-xylene as a shape controller, Adv. Mater. 18 (2006) 1883.
[30] I.E. Grey, M.J. Hardie, T.J. Ness, C.L. Raston, Octaphenylcyclotetrasiloxane confinement of C_{60} into double columnar arrays, Chem. Commun. (1999) 1139–1140.
[31] A. Talyzin, U. Jansson, C_{60} and C_{70} solvates studied by Raman spectroscopy, J. Phys. Chem. B 104 (2000) 5064–5071.
[32] M. Barrio, D.O. Lo´pez, J. Ll., P. Espeau Tamarit, R., H. Allouchi Ce´olin, Solid-state studies of C_{60} solvates formed in the $C_{60}-BrCCl_3$ system, Chem. Mater. 15 (2003) 288–291.
[33] R. Ce´olin, J.L. Tamarit, M. Barrio, D.O. Lo´pez, P. Espeau, H. Allouchi, R.J. Papoular, Solid state studies of the C_{60}. $2(CH_3)CCl_3$ solvate, Carbon 43 (2005) 417–424.
[34] H.B. Bürgi, R. Restori, D. Schwarzenbach, A.L. Balch, J.W. Lee, B.C. Noll, M.M. Olmstead, Nanocrystalline domains of a monoclinic modification of benzene stabilized in a crystalline matrix of C_{60}, Chem. Mater. 6 (1994) 1325–1329.
[35] H. He, J. Barras, J. Foulkes, J. Klinowski, Solid-state NMR studies of fullerene C_{60}/benzene solvates, J. Phys. Chem. B 101 (1997) 117–122.
[36] M.F. Meidine, P.B. Hitchcock, H.W. Kroto, R. Taylor, D.R.M. Walton, Single crystal X-ray structure of benzene-solvated C_{60}, J. Chem. Soc., Chem. Commun. (1992) 1534–1537.
[37] S. Pekker, G. Faigel, K. Fodor-Csorba, L. Gránásy, E. Jakab, M. Tegze, Structure and stability of crystalline C_{60}*n-pentane clathrate, Solid State Commun 83 (1992) 423–426.
[38] S. Toscani, H. Allouchi, J.L. Tamarit, D.O. Lo´pez, M. Barrio, V. Agafonov, V. Agafonov, A. Rassat, H. Szwarc, R. Ce´olin, Decagonal C_{60} crystals grown from *n*-hexane solutions: solid-state and aging studies, Chem. Phys. Lett. 330 (2000) 491–496.

[39] R. Ceolin, V. Agrafonov, B. Bachet, A. Gonthiervassal, H. Szwarc, S. Toscani, G. Keller, C. Fabre, A. Rassat, Solid-state studies on C_{60} solvates grown from *n*-heptane, Chem. Phys. Lett. 244 (1995) 100–104.

[40] X.D. Shi, A.R. Kortan, J.M. Williams, A.M. Kini, B.M. Savall, P.M. Chaikin, Sound velocity and attenuation in single-crystal C_{60}, Phys. Rev. Lett. 68 (1992) 827–830.

[41] K. Kikuchi, S. Suzuki, K. Saito, H. Shiromaru, A.A. Zakhidov, A. Ugawa, K. Imaeda, H. Inokuchi, K. Yakushi, Structure and superconductivity of single crystalline C_{60}, Physica C 185 (1991) 415–416.

[42] S.M. Gorun, K.M. Creegan, R.D. Sherwood, D.M. Cox, V.W. Day, C.S. Day, R. M. Upton, C.E. Briant, Solvated C_{60} and C_{60}/C_{70} and the low-resolution single crystal X-ray structure of C_{60}, J. Chem. Soc., Chem. Commun (1991) 1556–1558.

[43] A.L. Balch, J.W. Lee, B.C. Noll, M.M. Olmstead, Disorder in a crystalline form of buckminsterfullerene: C_{60}*$4C_6H_6$, J. Chem. Soc., Chem. Commun (1993) 56–58.

[44] A. Graja, R. Swietlik, Temperature study of IR-spectra of some C_{60} compounds, Synth. Met. 70 (1995) 1417–1418.

[45] R. Swietlik, P. Byszewski, E. Kowalska, Interactions of C_{60} with organic molecules in solvate crystals studied by infrared spectroscopy, Chem. Phys. Lett. 254 (1996) 73–78.

[46] B. Sundqvist Iwasiewicz-Wabnig, É. Kováts, I. Jalsovszky, S. Pekker, Polymerization of the rotor-stator compound C_{60}-cubane under high pressure, Phys. Rev. B: Condens. Matter 75 (2007) 024114.

[47] R. Röding Iwasiewicz-Wabnig, B. Sundqvist, É. Kováts, I. Jalsovszky, S. Pekker, Pressure–temperature phase diagram of the rotor-stator compound C_{60}-cube, Solid State Commun. 143 (2007) 208–212.

[48] K. Thirunavukkuarasu, C.A. Kuntscher, B.J. Nagy, I. Jalsovszky, G. Klupp, K. Kamarás, É. Kováts, S. Pekker, Orientational ordering and intermolecular interactions in the rotor-stator compounds C_{60}–C_8H_8 and C_{70}–C_8H_8 studied under high pressure, J. Phys. Chem. C 112 (2008) 17525–17532.

[49] C.A. Kuntscher, S. Frank, K. Kamarás, G. Klupp, É. Kováts, S. Pekker, G.y. Bényei, I. Jalsovszky, Pressure-dependent infrared spectroscopy on the fullerene rotor-stator compound C_{60}–C_8H_8, Phys. Status Solidi B 243 (2006) 2981–2984.

[50] E.A. Francis, G. Durkó, I. Jalsovszky, G. Klupp, K. Kamarás, É. Kováts, S. Pekker, C.A. Kuntscher, Phase transitions in C_{60}–C_8H_8 under hydrostatic pressure, Phys. Status Solidi B 249 (2012) 2596–2599.

[51] É. Kováts Iwasiewicz-Wabnig, S. Pekker, B. Sundqvist, Low-temperature optical studies of C_{60}-cubane rotor-stator compound, J. Phys. Conf. Ser. 100 (2008) 052091.

[52] A.V. Talyzin, L.S. Dubrovinsky, U. Jansson, High pressure Raman study of $C_{60}S_{16}$, Solid State Commun. 123 (2002) 93–96.

[53] K.P. Meletov, D.V. Konarev, Raman study of the pressure-induced charge transfer transition in the neutral donor–acceptor complexes $\{Ni(nPr_2dtc)_2\}(C_{60})_2$ and $\{Cu(nPr_2dtc)_2\}(C_{60})_2$. Fullerenes Nanotubes Carbon Nanostruct., 20:4-7, 336–340.

[54] K.P. Meletov, D.V. Konarev, Raman study of the pressure-induced phase transitions in the molecular donor-acceptor complex $\{Pt(dbdtc)_2\}C_{60}$, Chem. Phys. Lett. 553 (2012) 21–25.

[55] G. Sparn, J.D. Thompson, P.–M. Allemand, Q. Li, F. Wudl, K. Holczer, P.W. Stephens, Pressure dependence of magenetism in C_{60}TDAE, Solid State Commun. 82 (1992) 779–782.

[56] K. Mizoguchi, M. Machino, H. Sakamoto, T. Kawamotor, M. Tokumoto, A. Omerzu, D. Mihailovic, Pressure effect in TDAE-C_{60} ferromagnet: mechanism and polymerization, Phys. Rev. B: Condens. Matter 63 (2001) 140417.

[57] K. Mizoguchi, M. Takei, H. Sakamoto, T. Kawamotor, M. Tokumoto, A. Omerzu, D. Mihailovic, Uniaxial strain study in purely organic ferromagnet α-TDAE-C_{60}—mechanism and structure, Polyhedron 24 (2005) 2173–2175.

[58] L. Wang, B. Liu, H. Li, W. Yang, Y. Ding, S. Sinogeikin, Y. Meng, Z. Liu, X. Zeng., Ultra-incompressible Three Dimensional Long-range Ordered Amorphous Carbon Clusters, Science 337 (2012) 825 (–825).

[59] D.E.H. Jones, New Sci. 35 (1966) 245.

[60] D.E.H. Jones, The Inventions of Daedalus, W. H. Freeman, Oxford (1982) 118.

[61] R.S. Ruoff, A.L. Ruoff, Is C_{60} stiffer than diamond, Nature 350 (1991) 663–664.

[62] R.S. Ruoff, A.L. Ruoff, The bulk modulus of C_{60} molecules and crystals—a molecular mechanics approach, Appl. Phys. Lett. 59 (1991) 1553–1555.

[63] H.J. Mcskimin, W.L. Bond, Elastic moduli of diamond, Phys. Rev. 105 (1957) 116–121.

[64] J.E. Fischer, P.A. Heiney, A.R. McGhie, W.J. Romanow, A.M. Denenstein, J.P. McCauley Jr., A.B. Smith, Compressibility of solid C_{60}, Science 252 (1991) 1288–1290.

[65] L. Wang, B.B. Liu, D.D. Liu, M.G. Yao, S.D. Yu, Y.Y. Hou, T. Cui, G.T. Zou, B. Sundqvist, Z.J. Luo, H. Li, Y.C. Li, J. Liu, S.J. Chen, G.R. Wang, Y.C. Liu, Synthesis and high pressure induced amorphization of C_{60} nanosheets, Appl. Phys. Lett. 91 (2007) 103112.

[66] L. Wang, B.B. Liu, D.D. Liu, Y.Y. Hou, M.G. Yao, G.T. Zou, H. Li, Z.J. Luo, Y.C. Li, J. Liu, B. Sundqvist, High pressure studies of nano/sub-micrometer C-70 rods, High Energy Phys. Nucl. Phys. Chin. Ed. 29 (2005) 112–115.

[67] J.Y. Hu, N.N. Niu, G.Z. Piao, Y. Yang, Q. Zhao, Y. Yao, C.Z. Gu, C.Q. Jin, R.C. Yu, Phase transitions in single crystal tubes formed from C_{60} molecules under high pressure, Carbon 50 (2012) 5458–5462.

[68] J. Yang, C.L. Liu, C.X. Gao, In-situ electrical resistance and activation energy of solid C_{60} under high pressure, Chin. Phys. B 22 (2013) 096202.

[69] D.D. Liu, M.G. Yao, Q.J. Li, W. Cui, L. Wang, Z.P. Li, B. Liu, H. Lv, B. Zou, T. Cui, B. B. Liu, B. Sundqvist, In-situ Raman and photoluminescence study on pressure-induced phase transition in C_{60} nanotubes, J. Raman Spectrosc. 43 (2012) 737–740.

[70] D.D. Liu, M.G. Yao, L. Wang, Q.J. Li, W. Cui, B. Liu, R. Liu, B. Zou, T. Cui, B.B. Liu, J. Liu, B. Sundqvist, T. Wagberg, Pressure-induced phase transitions of C_{70} nanotubes, J. Phys. Chem. C 115 (2011) 8918–8922.

[71] L. Pintschovius, O. Blaschko, G. Krexner, N. Pyka, Bulk modulus of C_{60} studied by single-crystal neutron diffraction, Phys. Rev. B: Condens. Matter 59 (1999) 11020–11026.

[72] F. Moshary, N.H. Chen, I.F. Silvera, C.A. Brown, H.C. Dorn, M.S. de Vries, D.S. Bethune, Gap reduction and the collapse of solid C_{60} to a new phase of carbon under high pressure, Phys. Rev. Lett. 69 (1992) 466–469.

[73] H. Yanawaki, M. Yoshida, Y. Kakudate, S. Usuba, H. Yokoi, S. Fujiwara, K. Aoki, R. Ruoff, R. Malhotra, D. Lorents, Infrared study of vibrational property and polymerization of C_{60} and C_{70} under pressure, J. Phys. Chem. 97 (1993) 11161–11163.

[74] S.J. Duclos, K. Brister, R.C. Haddon, A.R. Kortan, F.A. Thiel, Effects of pressure and stress on C_{60} fullerite to 20 GPa, Nature 351 (1991) 380–382.

[75] V.A. Davydov, L.S. Kashevarova, A.V. Rakhmanina, V. Agafonov, H. Allouchi, R. Ce´olin, A.V. Dzyabchenko, V.M. Senyavin, H. Szwarc, T. Tanaka, K. Komatsu, Particularities of C_{60} Transformations at 1.5 GPa, J. Phys. Chem. B 103 (1999) 1800–1804.

[76] Y. Iwasa, T. Arima, R.M. Fleming, T. Siegrist, O. Zhou, R.C. Haddon, L.J. Rothberg, K.B. Lyons, H.L. Carter, A.F. Hebard, R. Tycko, G. Dabagh, J.J. Krajewski, G.A. Thomas, T. Yagi, New phases of C_{60} synthesized at high pressure, Science 264 (1994) 1570–1572.

[77] I.O. Bashkin, V.I. Rashchupkin, A.F. Gurov, A.P. Moravsky, O.G. Rybchenko, N.P. Kobelev, Y.M. Soifer, E.G. Ponyatovskii, A new phase transition in the T–P diagram of C_{60} fullerite, J. Phys. Condens. Matter 36 (1994) 7491.

[78] P.A. Persson, U. Edlund, P. Jacobsson, D. Johnels, A. Soldatov, B. Sundqvist, NMR and Raman characterization of pressure polymerized C_{60}, Chem. Phys. Lett. 258 (1996) 540–546.

[79] M. Nunez-Regueiro, L. Marques, J.L. Hodeau, O. Bethoux, M. Perroux, Polymerized fullerite structures, Phys. Rev. Lett. 74 (1995) 278–281.

[80] L.A. Chernozatonskii, N.R. Serebryanaya, The superhard crystalline three-dimensional polymerized C_{60} phase, Chem. Phys. Lett. 316 (2000) 199–204.

[81] N.R. Serebryanaya, L.A. Chernozatonskii, Modelling and interpretation of the experimental data on the 3D polymerized C_{60} fullerites, Solid State Commun. 114 (2000) 537–541.

[82] L. Marques, M. Mezouar, J.-L. Hodeau, M. Núñez-Regueiro, N.R. Serebryanaya, V.A. Ivdenko, V.D. Blank, G.A. Dubitsky, Debye–Scherrer Ellipses from 3D fullerene polymers: an anisotropic pressure memory signature, Science 283 (1999) 1720–1723.

[83] M. Mezouar, L. Marques, J.-L. Hodeau, V. Pischedda, M. Núñez-Regueiro, Equation of state of an anisotropic three-dimensional C_{60} polymer: the most stable form of fullerene, Phys. Rev. B: Condens. Matter 68 (2003) 193414.

[84] V.D. Blank, S.G. Buga, G.A. Dubitsky, N.R. Serebryanaya, S.N. Sulyanov, M.Y.u. Popov, in: Molecular Nanostructures, (Ed.) H. Kuzmany, J. Fink, M. Mehring and S. Roth. World Scientific, Singapore, 1998 pp. 506–510.

[85] V.D. Blank, S.G. Buga, N.R. Serebryanaya, V.N. Denisov, G.A. Dubitsky, A.N. Ivlev, B.N. Mavrin, M.Y.u. Popov, Ultrahard and superhard carbon phases produced from C_{60} by heating at high pressure: structural and Raman studies, Phys. Lett. A 205 (1995) 208–216.

[86] V.D. Blank, S.G. Buga, G.A. Dubitsky, N.R. Serebryanaya, V.N. Denisov, A.N. Ivlev, B.N. Mavrin, M.Y.u. Popov, Synthesis of ultrahard and superhard materials from C_{60} fullerite, Mol. Cryst. Liq. Cryst. Sci. Technol., Sect. C 7 (1996) 251–256.

[87] S. Wasa, K. Suito, M. Kobayashi, A. Onodera, Pressure-induced irreversible amorphization of C_{70} fullerene, Solid State Commun. 114 (2000) 209–213.

[88] S. Lebedkin, W.E. Hull, A.V. Soldatov, B. Renker, M.M. Kappes, J. Phys. Chem. B 104 (2000) 4101.

[89] A.V. Soldatov, G. Roth, A. Dzyabchenko, D. Johnels, S. Lebedkin, C. Meingast, B. Sundqvist, M. Haluska, H. Kuzmany, Science 293 (2001) 860.

[90] V.D. Blank, N.R. Serebryanaya, G.A. Dubitsky, S.G. Buga, V.N. Denisov, B.N. Mavrin, I.N. Ivlev, S.N. Sulyanov, N.A. Lvova, Phys. Lett. A 248 (1998) 415.

[91] R.S. Ruoff, D.S. Tse, R. Malhotra, D.C. Lorents, Solubility of C_{60} in a variety of solvents, J. Phys. Chem. 97 (1993) 3379–3383.

[92] A. Demortier, R. Doome, A. Fonseca, J.B. Nagy, Study of the anomalous solubility behavior of solutions saturated with fullerenes by C13-NMR, Magn. Reson. Colloid Interface Sci.—NATO Sci. Series 76 (2002) 513–518.

[93] R.E. Haufler, J. Conceicao, L.P.F. Chibante, Y. Chai, N.E. Byrne, S. Flanagan, M.M. Haley, S.C. Obrien, C. Pan, Z. Xiao, W.E. Billups, M.A. Ciufolini, R. H. Hauge, J.L. Margrave, L.J. Wilson, R.F. Curl, R.E. Smalley, Efficient production of C_{60} (Buckminsterfullerene), $C_{60}H_{36}$, and the solvated buckide ion, J. Phys. Chem. 94 (1990) 8634–8636.

[94] M.V. Korobov, E.B. Stukalin, A.L. Mirakyan, I.S. Neretin, Y.L. Slovokhotov, A.V. Dzyabchenko, A.I. Ancharov, B.P. Tolochko, New solid solvated of C_{60} and C_{70} fullerenes: the relationship between structures and lattice energies, Carbon 41 (2003) 2743–2755.

[95] A.K. Gangopadhyay, J.S. Schilling, M.D. Leo, W.E. Buhro, K. Robinson, T. Kowalewski, Synthesis and characterization of $C_{60}[CCl_4]_{10}$, Solid State Commun. 96 (1995) 597–600.

[96] C. Collins, J. Foulkes, A.D. Bond, J. Klinowski, Crystalline C_{60}*$2CHBr_3$: a solid-state study, Phys. Chem. Chem. Phys. 1 (1999) 5323–5326.

[97] R. Ceolin, J.L.1 Tamarit, M. Barrio, D.O. Lopez, S. Toscani, H. Allouchi, V. Agafonov, H. Szwarc, Solid-state studies on a cubic 1:1 solvate of C_{60}

grown from dichloromethane and leading to another hexagonal C_{60} polymorph, Chem. Mater. 13 (2001) 1349–1355.
[98] P. Espeau, M. Barrio, D.O. Lopez, J.L.1 Tamarit, R. Ceolin, H. Allouchi, V. Agafonov, F. Masin, H. Szwarc, Phase equilibria in the C_{60}+Ferrocene system and solid-state studies of the C_{60}*2Ferrocene solvate, Chem. Mater. 14 (2002) 321–326.
[99] M. Barrio, D.O. Lopez, J.L.1 Tamarit, P. Espeau, R. Ceolin, H. Allouchi, Solid-state studies of C_{60} solvates formed in the C_{60}–$BrCCl_3$ system, Chem. Mater. 15 (2003) 288–291.
[100] R. Ceolin, D.O. Lopez, M. Barrio, J.L.1 Tamarit, P. Espeau, B. Nicolai, H. Allouchi, R. Papoular, Solid state studies on C_{60} solvates formed with *n*-alcanes: orthorhombic C_{60}*2/3*n*-nonane, Chem. Phys. Lett. 399 (2004) 401–405.
[101] M.M. Olmstead, L.J. Hao, A.L. Balch, Preparation and crystallographic studies of $C_{70}Pd(PPh_3)_2$*CH_2Cl_2 and C_{70}*2($(C_5H_5)_2Fe$), J. Organomet. Chem. 578 (1999) 85–90.
[102] C. Park, E. Yoon, M. Kawano, T. Joo, H.C. Choi, Self-crystallization of C_{70} cubes and remarkable enhancement of photoluminescence, Angew. Chem. Int. Ed. 49 (2010) 9670–9675.
[103] S. Pekker, É. Kováts, G. Oszlányi, G. Bényei, G. Klupp, G. Bortel, I. Jalsovszky, E. Jakab, F. Borondics, K. Kamarás, M. Bokor, G. Kriza, K. Tompa, G. Faigel, Rotor–stator molecular crystals of fullerenes with cubane, Nat. Mater. 4 (2005) 764–767.
[104] G. Bortel, G. Faigel, É. Kováts, G. Oszlányi, S. Pekker, Structural study of C_{60} and C_{70} cubane, Phys. Status Solidi B 243 (2006) 2999–3003.
[105] A. Talyzin, U. Jansson, Preparation and characterization of $C_{60}S_{16}$ and $C_{70}S_{48}$ thin films, Thin Solid Films 350 (1999) 113–118.
[106] F. Masin, A.–S. Grell, I. Messari, G. Gusman, Benzene-solvated C_{60}: 1H nuclear spin-lattice magnetic relaxation, Solid State Commun. 106 (1998) 59–62.
[107] M.G. Yao, W. Cui, J.P. Xiao, S.L. Chen, J.X. Cui, R. Liu, T. Cui, B. Zou, B.B. Liu, B. Sundqvist, Pressure-induced transformation and superhard phase in fullerenes: the effect of solvent intercalation, Appl. Phys. Lett. 103 (2013) 071913.
[108] W. Cui, M.G. Yao, D.D. Liu, Q.J. Li, R. Liu, B. Zou, T. Cui, B.B. Liu, Reversible polymerization in doped fullerides under pressure: the case of $C_{60}(Fe(C_5H_5)_2)_2$, J. Phys. Chem. B 116 (2012) 2643–2650.
[109] W. Cui, M.G. Yao, Z. Yao, F.X. Ma, Q.J. Li, R. Liu, B. Liu, B. Zou, T. Cui, B.B. Liu, B. Sundqvist, Reversible pressure-induced polymerization of $Fe(C_5H_5)_2$ doped C_{70}, Carbon 62 (2013) 447–454.
[110] K. Mizoguchi, M. Takei, M. Machino, H. Sakamoto, M. Tokumoto, T. Kawamoto, A. Omerzu, D. Mihailovic, Magnetism of α- and β-TDAE-C_{60}, J. Magn. Magn. Mater. 272 (2004) E215.
[111] D. Arčon, R. Blinc, P. Cevc, A. Omerzu, Evidence for S=0-type spin pairing in the nonferromagnetic modification of TDAE−C_{60}, Phys. Rev. B: Condens. Matter 59 (1999) 5247.